

Article

## Effects of Salt Additives to the KOH Electrolyte Used in Ni/MH Batteries

Suli Yan <sup>1,†</sup>, Kwo-Hsiung Young <sup>1,2,\*</sup> and K.Y. Simon Ng <sup>1,†</sup>

<sup>1</sup> Department of Chemical Engineering and Materials Science, Wayne State University, Detroit, MI 48202, USA; E-Mails: shuliyuan2010@gmail.com (S.Y.); simonng2008@gmail.com (K.Y.S.N.)

<sup>2</sup> BASF/Battery Materials-Ovonic, 2983 Waterview Drive, Rochester Hills, MI 48309, USA

<sup>†</sup> These authors contributed equally to this work.

\* Author to whom correspondence should be addressed; E-Mail: kwo.young@basf.com; Tel.: +1-248-293-7000; Fax: +1-248-299-4228.

Academic Editor: Joeri Van Mierlo

Received: 21 September 2015 / Accepted: 18 November 2015 / Published: 27 November 2015

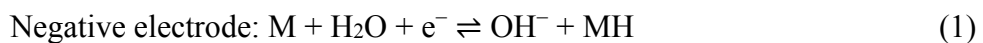
**Abstract:** KOH-based electrolytes with different salt additives were investigated to reduce their corrosive nature toward Mg/Ni metal hydride alloys used as negative electrodes in nickel metal hydride (Ni/MH) batteries. Alkaline metal halide salts and oxyacid salts were studied as additives to the traditional KOH electrolyte with concentrations varying from 0.005 M to 1.77 M. Effects of the cations and anions of the additives on charge/discharge performance are discussed. The reduction potential of alkaline cations and radii of halogen anions were correlated with initial capacity and degradation of the metal hydride alloy. A synergistic effect between KOH and some oxyacid salt additives was observed and greatly influenced by the nature of the salt additives. It was suggested that both the formation of a solid film over the metal hydride surface and the promotion of proton transfer in the additives containing electrolytes led to a decreased degradation of the electrodes and an increased discharge capacity. 12 salt additives, NaC<sub>2</sub>H<sub>3</sub>O<sub>2</sub>, KC<sub>2</sub>H<sub>3</sub>O<sub>2</sub>, K<sub>2</sub>CO<sub>3</sub>, Rb<sub>2</sub>CO<sub>3</sub>, Cs<sub>2</sub>CO<sub>3</sub>, K<sub>3</sub>PO<sub>4</sub>, Na<sub>2</sub>WO<sub>4</sub>, Rb<sub>2</sub>SO<sub>4</sub>, Cs<sub>2</sub>SO<sub>4</sub>, NaF, KF, and KBr, were found to increase the corrosion resistance of the MgNi-based metal hydride alloy.

**Keywords:** nickel metal hydride (Ni/MH) battery; electrolyte additives; corrosion; MgNi based anodes; alkaline halides

## 1. Introduction

Nickel metal hydride (Ni/MH) batteries are currently one of the most widely used energy storage devices with many applications including hybrid electric vehicles, vacuum cleaners, electric toys, power tools, cordless phones, *etc.* [1,2]. They have many advantages such as having a high specific power, excellent tolerance to abuse, long cycle life, wide temperature operation range, and low self-discharge. Facing competition from Li-ion batteries, scientists continue to improve the various properties of Ni/MH batteries. One of the key areas demanding immediate attention is the gravimetric energy density.

A basic Ni/MH battery consists of an assembly of a highly conductive electrolyte, a metal hydride (MH) negative electrode, and a nickel hydroxide positive electrode. The cell reactions on the electrodes are shown in following equations:



The most widely used electrolytes are pure KOH aqueous solutions with concentrations in the range of 20–36 wt% because these solutions are highly conductive and can efficiently convey protons in an electric field. AB<sub>5</sub> and A<sub>2</sub>B<sub>7</sub> type MH alloys with electrocapacity in the range of 300–350 mAh·g<sup>-1</sup> have been commercialized as the negative electrodes for a long time. For the positive electrode, β-Ni(OH)<sub>2</sub> co-precipitated with Co and Zn with an energy density of about 240 mAh·g<sup>-1</sup> is the most commonly used material.

During charge, a negative voltage (with respect to the counter electrode) is applied to the MH electrode, and electrons enter the metal through the current collector to neutralize the protons produced from the splitting of water that occurs at the metal/electrolyte interface. During discharge, protons in the MH leave the surface and recombine with OH<sup>-</sup> in the alkaline electrolyte to form H<sub>2</sub>O and the resulting charge neutrality pushes the electrons out of the MH through the current collector, performing electrical work in the outer circuitry. Due to their demanding applications in Ni/MH batteries, MH alloys are required to possess a high capacity and moderate hydride stability. Iwakura *et al.* [3] and Geng *et al.* [4] tested the pressure-composition-temperature (P-C-T) isotherm curves of MH alloys, and correlated the hydrogen content with electrochemical potential through the Nernst equation. It was found that higher hydrogen content of alloys lead to higher electrochemical capacity. A wide set of hydrogen storage electrode alloys, other than AB<sub>5</sub> and A<sub>2</sub>B<sub>7</sub> type, have been reported to contain high hydrogen content and high electrochemical capacity. Among them, MgNi-based amorphous and nanocrystalline MH alloys are reported to have higher capacity than those in AB<sub>5</sub> and A<sub>2</sub>B<sub>7</sub> [5,6]. For example, Young and Nei [7] reported that the theoretical capacity of MgNi metal alloys is about 1080 mAh·g<sup>-1</sup> and Anik *et al.* [8] reported that the practical electrocapacity values of MgNi and Mg<sub>0.9</sub>Mo<sub>0.1</sub>Ni (M = B, Ti, and Zr) type alloys are up to 495 mAh·g<sup>-1</sup> and 508 mAh·g<sup>-1</sup>, respectively. The theoretical capacities of Mg<sub>80</sub>Sc<sub>20</sub>, Mg<sub>80</sub>Ti<sub>20</sub>, Mg<sub>80</sub>V<sub>20</sub>, and Mg<sub>80</sub>Cr<sub>20</sub> reach 1790, 1750, 1700, and 1270 mAh·g<sup>-1</sup>, respectively. High hydrogen storage capacity, light weight, and the low cost of Mg type alloys make them one of the most promising commercially viable materials for high capacity Ni/MH batteries.

However, as many researchers have stated, MgNi-based electrodes are still far from commercial application because of the rapid decay of electrochemical capacity. Rongeat *et al.* [9] reported a 70%

decay in capacity after 20 charge/discharge cycles. A lot of effort has been put into increasing the corrosion resistance of MgNi-based alloys to KOH electrolytes, mostly through studying various types of substitutions in the MgNi formula, such as replacements of the A- (by rare earth, transition, or other metals [10]) and B-sites (by transition metals [11,12]), different fabrication procedures [13], and surface treatment [14].

It is well known that the use of electrolyte additives is one of the most economic and effective methods to improve the performance of electrodes as they do not affect the gravimetric and volumetric energy density of the battery. However, there are only a few studies of the modification of traditional KOH electrolytes to improve the cycle life of Ni/MH batteries. For example, Danczuk *et al.* [15] and Karwowska *et al.* [16] studied the effects of alkaline cation additives in KOH electrolyte to AB<sub>5</sub> type alloys; Shangguan *et al.* [17] found that Na<sub>2</sub>WO<sub>4</sub> additives could increase the high temperature performance of Ni electrodes; Vaidyanathan *et al.* [18] reported that KSiO<sub>4</sub> and KNO<sub>3</sub> additives could increase the end-of-charge voltage for Ni/MH batteries. Until now, very few studies for electrolyte additives' effects to MgNi-based Ni/MH batteries have been reported. In this study, a systematic investigation on the effect of salt additives to the performance of traditional KOH electrolyte to an Mg<sub>52</sub>Ni<sub>39</sub>Co<sub>3</sub>Mn<sub>6</sub> alloy prepared by the melt-spin and consequently mechanical alloying is performed. The experiment is accomplished by partially replacing KOH in the traditional electrolyte with salt additives while keeping the total ionic concentrations the same; thus, a better understanding of the effect of the anion and cation substitute of KOH electrolyte in Ni/MH battery can be obtained. The ultimate objective of this study is to develop a novel salt containing electrolyte formulation, which is as highly conductive as the traditional KOH electrolyte, but less corrosive to MgNi-based negative electrodes. With this new electrolyte, MgNi-based NiMH battery is expected to have the same, or even higher, electrochemical capacity and improved capacity stability compared to the traditional 30 wt% KOH electrolyte. The mechanism for proton transfer and improved corrosion resistance is also briefly discussed in this work.

## 2. Experimental

### 2.1. Materials and Electrolyte Matrix

The MgNi alloy (Mg<sub>52</sub>Ni<sub>39</sub>Co<sub>3</sub>Mn<sub>6</sub>) was provided by BASF/Battery Materials-Ovonic, Rochester Hills, MI, USA. The alloy was prepared by melt-spin followed by mechanical alloying. Details of the alloy preparation were described elsewhere [19]. Sintered  $\beta$ -Ni(OH)<sub>2</sub> was also obtained from BASF/Battery Materials-Ovonic. The matrix examined on the effects of salt additives in aqueous KOH solution consisted of the following: (1) alkaline salts, including LiCl, NaCl, KCl, RbCl, and CsCl (with salt concentrations at 0.44, 0.88, 1.33, and 1.77 M each and KOH concentrations change accordingly as 6.33, 5.88, 5.44, and 5.00 M, respectively, with the total ionic concentration kept at 6.77 M); (2) halogen containing salts including KF, KCl, KBr, and KI (with salt concentrations the same as previously mentioned); (3) oxyacid containing salts, including LiNO<sub>3</sub>, NaNO<sub>3</sub>, KNO<sub>3</sub>, RbNO<sub>3</sub>, CsNO<sub>3</sub>, K<sub>2</sub>CO<sub>3</sub>, Na<sub>2</sub>CO<sub>3</sub>, Cs<sub>2</sub>CO<sub>3</sub>, Rb<sub>2</sub>CO<sub>3</sub>, K<sub>3</sub>PO<sub>4</sub>, KIO<sub>4</sub>, Li<sub>2</sub>SO<sub>4</sub>, K<sub>2</sub>SO<sub>4</sub>, Na<sub>2</sub>SO<sub>4</sub>, Rb<sub>2</sub>SO<sub>4</sub>, Cs<sub>2</sub>SO<sub>4</sub>, LiCHO<sub>2</sub>, NaCHO<sub>2</sub>, KCHO<sub>2</sub>, CsCHO<sub>2</sub>, Na<sub>2</sub>WO<sub>4</sub>, NaC<sub>2</sub>H<sub>3</sub>O<sub>2</sub>, and KC<sub>2</sub>H<sub>3</sub>O<sub>2</sub> (with salt concentration at 0.44 M and 6.33 M KOH each for LiNO<sub>3</sub>, NaNO<sub>3</sub>, KNO<sub>3</sub>, RbNO<sub>3</sub>, CsNO<sub>3</sub>, KIO<sub>4</sub>, LiCHO<sub>2</sub>, NaCHO<sub>2</sub>, KCHO<sub>2</sub>,

$\text{CsCHO}_2$ ,  $\text{NaC}_2\text{H}_3\text{O}_2$ , and  $\text{KC}_2\text{H}_3\text{O}_2$ ; 0.29 M and 6.33 M KOH each for  $\text{K}_2\text{CO}_3$ ,  $\text{Na}_2\text{CO}_3$ ,  $\text{Cs}_2\text{CO}_3$ ,  $\text{Rb}_2\text{CO}_3$ ,  $\text{Na}_2\text{WO}_4$ ; 0.005 M and 6.33 M KOH each for  $\text{Li}_2\text{SO}_4$ ,  $\text{K}_2\text{SO}_4$ ,  $\text{Na}_2\text{SO}_4$ ,  $\text{Rb}_2\text{SO}_4$ , and  $\text{Cs}_2\text{SO}_4$ ; and 0.22 M salt and 6.33 M KOH for  $\text{K}_3\text{PO}_4$ ); (4) other salts, including  $\text{NaF}$ ,  $\text{LiBr}$ , and  $\text{NaBr}$  with salt concentration at 0.44 M and 6.33 M KOH each. All salt additives were purchased from Sigma-Aldrich Company (St. Louis, MO, USA). Except for the  $\text{SO}_4^{2-}$  containing electrolytes, the total ion concentration of all electrolytes is kept at 13.54 M.

## 2.2. Measurements and Calculations

Electrochemical charge/discharge cycling tests were performed with an Arbin BT2000 battery tester (Arbin Instrument, College Station, TX, USA) at room temperature. For the test cells, the positive electrode was the sintered  $\beta\text{-Ni(OH)}_2$  and the negative electrode was made from directly dry-compacting the MgNi-based  $\text{Mg}_{52}\text{Ni}_{39}\text{Co}_3\text{Mn}_6$  alloy onto the Ni-expanded metal without using any binder. A hydrophilic nonwoven polyolefin was used as the separator. The cell was charged at  $100 \text{ mA} \cdot \text{g}^{-1}$  for 5 h, and discharged first at  $100 \text{ mA} \cdot \text{g}^{-1}$  to reach a cut-off voltage fixed at 0.9 V. This is followed by resting for 30 s and the voltage will be recovered to a higher value, and then discharged at  $24 \text{ mA} \cdot \text{g}^{-1}$  to reach a cut-off voltage fixed at 0.9 V. The process is repeated by a final discharge at  $8 \text{ mA} \cdot \text{g}^{-1}$  to 0.9 V. The conductivity of the electrolyte was analyzed by an YSI model 3200 conductivity meter with a probe produced by Traceable VWR Inc. (West Chester, PA, USA). Cell is considered failed when its capacity drops below 70% of the initial capacity before cycling.

Three parameters: conductivity, discharge capacity, and degradation, were measured and compared to those with traditional 30% KOH electrolyte. Each test was repeated three times. Degradation was determined as the percent capacity loss per cycle within the initial 10 cycles, as shown in the following:

$$\text{Degradation \%} = \frac{\frac{\text{Cap}_{\text{high}} - \text{Cap}_{\text{low}}}{(n_{\text{high}} - n_{\text{low}}) \times \text{Cap}_{\text{high}}}}{\frac{\text{Cap}_{0,\text{high}} - \text{Cap}_{0,\text{low}}}{(n_{0,\text{high}} - n_{0,\text{low}}) \times \text{Cap}_{0,\text{high}}}} \times 100\% \quad (3)$$

where:

$\text{Cap}_{\text{high}}$  is the highest value of discharge capacity in the initial 10 cycles;

$\text{Cap}_{\text{low}}$  is the lowest value of discharge capacity in the initial 10 cycles;

$n_{\text{high}}$  is the cycle number of the highest discharge capacity in the initial 10 cycles;

$n_{\text{low}}$  is the cycle number of the lowest discharge capacity in the initial 10 cycles;

Subscript 0 is for 6.77 M (30%) KOH electrolyte.

## 3. Results and Discussion

### 3.1. Electrochemical Performance of MgNi-Based NiMH with 30% KOH Electrolyte

The cycle stability and capacity/degradation as functions of KOH concentration of negative electrode composed of  $\text{Mg}_{52}\text{Ni}_{39}\text{Co}_3\text{Mn}_6$  MH alloy in a traditional 30% KOH electrolyte are shown in Figures 1 and 2, respectively. This composition is selected due to its weak resistance to corrosion in traditional alkaline electrolyte, which allows for a better comparison of the effectiveness of additives.

Other MgNi MH alloy compositions with high capacities and better cycle stability in 30% KOH are also available but were not used in this work. Figure 1 depicts the discharge capacities of  $\text{Mg}_{52}\text{Ni}_{39}\text{Co}_3\text{Mn}_6$  in the first 10 cycles at five different KOH concentrations: 6.77, 6.33, 5.88, 5.44, and 5.00 M. It shows a rapid decay of discharge capacity in the first four cycles for all KOH concentrations and the capacity loss is more than 80% after 10 cycles. This result is consistent with other reported MgNi-based MH alloys [9]. Figure 2 shows the normalized capacity and degradation as functions of KOH concentration. A low KOH concentration corresponds to a low degradation; however, a low discharge capacity as well. Therefore, it is necessary to balance the degradation and discharge capacity of negative electrode by a matrix of salt additives.

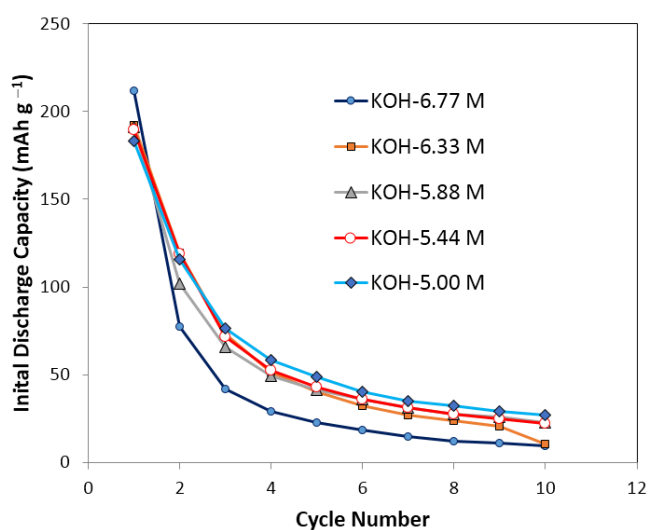


**Figure 1.** Initial discharge capacity of pure KOH solutions in initial 10 cycles. KOH concentrations are 6.77 M, 6.33 M, 5.88 M, 5.33 M, and 5.00 M separately. It shows a decay of discharge capacity for more than 80% after 10 cycles' running for all the pure KOH electrolytes.

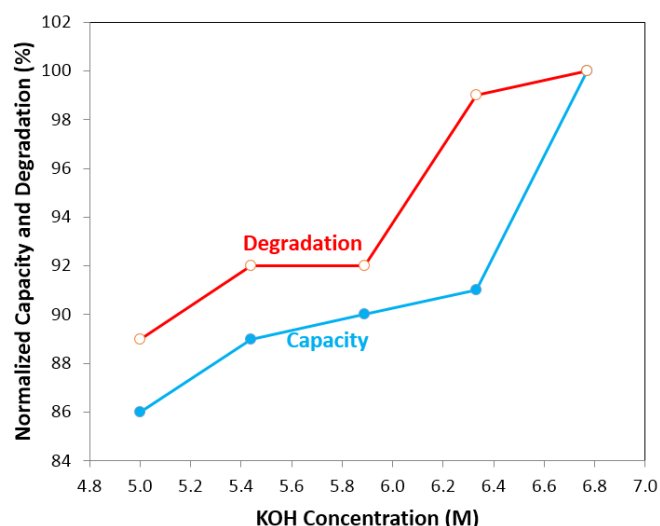


**Figure 2.** Capacity and degradation of pure KOH electrolytes vs. KOH concentration. It shows at low KOH concentration, electrolyte has low degradation but low discharge capacity; at high KOH concentration, electrolyte has a high discharge capacity but high degradation.

### 3.2. Electrochemical Performance of Pure Salt Solutions

The conductivity, capacity, and degradation characteristics of KOH and various pure salt solutions are shown in Table 1. For a 6.77 M KOH electrolyte, the cells were cycled for more than 20 cycles with the total charging/discharging time of more than 130 h before cell failure. However, most of the cells with pure salt solutions as electrolyte totally lost activity within the first few cycles. For example, the cells with a 1.77 M LiCl solution lost all electrochemical activity only after five cycles. The cells were disassembled after the test and both the MgNi-based MH alloy and nickel hydroxide electrodes were found to be heavily corroded. Table 1 also shows that the conductivities of pure salt solutions are less than 20% of the conductivity of 6.77 M KOH electrolytes. Low conductivities could cause a low electronic efficiency for Ni/MH battery systems. Most of the pure salt solutions have a higher degradation compared to KOH, as shown in Table 1. While some salt solutions such as KF and RbCl resulted in a lower degradation, their capacities decreased significantly, which can be attributed to low electronic efficiencies. Table 1 indicates that all of the pure salt solutions were more corrosive to the electrodes than the standard KOH solution and are therefore unsuitable as electrolytes for Ni/MH systems.

**Table 1.** Test time, test cycles, capacity, degradation and conductivity of pure 6.77 M KOH solution, pure 1.77 M salt solutions. The salts include KF, KCl, KBr, KI, LiCl, NaCl, KCl, RbCl, and CsCl. Note that the high corrosion could be observed in pure salt solutions.

Salt	Concentration in M	Test time before cell failed in h	Test cycles before cell failed	Capacity % <sup>1</sup>	Degradation % <sup>2</sup>	Conductivity % <sup>3</sup>
KOH	6.77	>130	>20	100.0	100.0	100.0
KF	1.77	105	20	12.3	49.4	12.9
KCl	1.77	73	8	79.7	136.5	14.6
KBr	1.77	56	4	167.4	309.9	12.9
KI	1.77	128	20	16.3	n/a	15.0
LiCl	1.77	56	5	84.7	185.4	10.3
NaCl	1.77	100	11	100.0	121.2	12.0
KCl	1.77	73	8	79.7	136.5	14.6
RbCl	1.77	70	9	82.8	88.8	15.0
CsCl	1.77	42	4	79.4	105.0	14.2

<sup>1</sup>: test error for capacity is 10%; <sup>2</sup>: test error for degradation is 10%; <sup>3</sup>: test error for conductivity is 5%.

### 3.3. Electrochemical Performance of Mixtures of Salt and KOH Solutions

#### 3.3.1. Effect of Salt Additives on Conductivity

Traditionally, the concentration of KOH used in commercial Ni/MH batteries varies from 4.1 M to 8.5 M. Thus, the conductivities of KOH electrolytes with concentrations of 4.15, 4.65, 5.15, 5.67, 6.21, 6.77, 7.33, 7.91, and 8.52 M were tested. If we normalize the conductivities to the conductivity of 6.77 M KOH electrolyte as 100%, the conductivities of each of the electrolytes varied from 88% to 100%, as shown in Table 2.

**Table 2.** Conductivity of traditional KOH electrolyte with concentration varies from 20 wt% to 36 wt%. Note the conductivities vary from 88% to 100%.

Sample number	KOH concentration in M	Normalized conductivity in % <sup>1</sup>
1	4.15	88.2
2	4.64	92.6
3	5.15	95.6
4	5.67	98.5
5	6.21	98.5
6	6.77	100.0
7	7.33	95.6
8	7.91	92.6
9	8.52	89.7

<sup>1</sup>: test error for normalized conductivity is 5%.

Electrolytes containing 6.33 M KOH and 32 types of salt additives were prepared and their conductivities were tested and shown in Table 3. It was found that the conductivities of all the additive-containing electrolytes vary from 88% to 100%. It shows that the salt containing electrolytes can be as conductive as traditional KOH electrolytes in some cases (KIO<sub>4</sub> and KNO<sub>3</sub>).

**Table 3.** Conductivity and concentration of additive containing electrolyte. Note the conductivities vary from 88% to 100%.

Salt	Concentration in M	Conductivity in % <sup>1</sup>	Salt	Concentration in M	Conductivity in % <sup>1</sup>	Salt	Concentration in M	Conductivity in % <sup>1</sup>
LiCl	0.44	97.4	Na <sub>2</sub> WO <sub>4</sub>	0.29	88.3	Li <sub>2</sub> SO <sub>4</sub>	0.005	90.7
NaCl	0.44	97.4	KIO <sub>4</sub>	0.44	100.0	Na <sub>2</sub> SO <sub>4</sub>	0.005	91.4
KCl	0.44	97.0	LiNO <sub>3</sub>	0.44	97.7	K <sub>2</sub> SO <sub>4</sub>	0.005	89.0
RbCl	0.44	96.3	NaNO <sub>3</sub>	0.44	97.7	Rb <sub>2</sub> SO <sub>4</sub>	0.005	89.3
CsCl	0.44	96.3	RbNO <sub>3</sub>	0.44	95.5	Cs <sub>2</sub> SO <sub>4</sub>	0.005	88.7
KF	0.44	96.8	KNO <sub>3</sub>	0.44	100	LiCHO <sub>2</sub>	0.44	92.4
KBr	0.44	98.3	K <sub>2</sub> CO <sub>3</sub>	0.29	99.6	KCHO <sub>2</sub>	0.44	93.6
KI	0.44	96.1	Cs <sub>2</sub> CO <sub>3</sub>	0.29	97.0	CsCHO <sub>2</sub>	0.44	94.1
LiBr	0.44	93.8	Rb <sub>2</sub> CO <sub>3</sub>	0.29	98.5	KC <sub>2</sub> H <sub>3</sub> O <sub>2</sub>	0.44	89.4
NaBr	0.44	94.5	Na <sub>2</sub> CO <sub>3</sub>	0.29	89.0	NaC <sub>2</sub> H <sub>3</sub> O <sub>2</sub>	0.44	90.5
NaF	0.44	96.9	K <sub>3</sub> PO <sub>4</sub>	0.22	99.2	-	-	-

<sup>1</sup>: test error for conductivity is 5%.

### 3.3.2. Effect of Salt Additives on Discharge Capacity and Degradation

Figure 3 shows the effects of the salt additive containing electrolytes on the discharge capacity and degradation. Data are normalized to the degradation and discharge capacity of 6.77 M KOH. Figure 3 can be divided into four different areas depending on the degradation and capacity.

Area 1: normalized degradation <100% and normalized capacity >100%. The electrolytes in this area are the most desirable since they offer lower degradations with improved capacities. It includes NaC<sub>2</sub>H<sub>3</sub>O<sub>2</sub> (0.44 M and 6.33 M KOH solution), KC<sub>2</sub>H<sub>3</sub>O<sub>2</sub> (0.44 M and 6.33 M KOH solution),

$\text{K}_2\text{CO}_3$  (0.29 M and 6.33 M KOH, 0.59 M and 5.88 M KOH, 0.89 M and 5.44 M KOH solutions),  $\text{Rb}_2\text{CO}_3$  (0.29 M and 6.33 M KOH solution),  $\text{Cs}_2\text{CO}_3$  (0.29 M and 6.33 M KOH solution),  $\text{K}_3\text{PO}_4$  (0.22 M and 6.33 M KOH, 0.44 M and 5.88 M KOH, 0.66 M and 5.44 M KOH, 0.88 M and 5 M KOH solutions),  $\text{NaF}$  (0.44 M and 6.33 M KOH solution), KF (0.44 M and 6.33 M KOH, 0.88 M and 5.88 M KOH solutions),  $\text{NaBr}$  (0.44 M and 6.33 M KOH solution),  $\text{Rb}_2\text{SO}_4$  (0.005 M and 6.33 M KOH solution),  $\text{Cs}_2\text{SO}_4$  (0.005 M and 6.33 M KOH solution), KBr (0.44 M and 6.33 M KOH solution), LiBr (0.44 M and 6.33 M KOH solution), and  $\text{RbCl}$  (0.88 M and 5.88 M KOH solution).

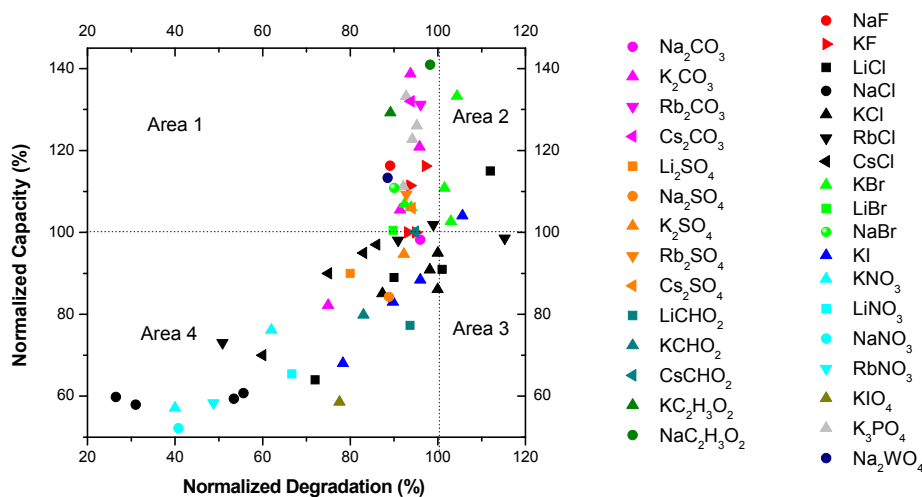


**Figure 3.** Screen test results of discharge capacity and degradation for the electrolytes containing various salt additives.

Area 2: normalized degradation >100% and normalized capacity >100%. This area contains electrolytes with chemical activity which increase both the capacity and the degradation of the MgNi-based MH alloy. KBr (0.88 M and 5.88 M KOH, 1.33 M and 5.44 M KOH, 1.77 M and 5 M KOH solutions),  $\text{LiCl}$  (0.44 M and 6.33 M KOH solution), and KI (0.44 M and 6.33 M KOH solution) are examples.

Area 3: normalized degradation >100% and normalized capacity <100%. It includes  $\text{RbCl}$  (1.33 M and 5.44 M KOH solution),  $\text{LiCl}$  (0.88 M and 5.88 M KOH solution), and KCl (0.44 M and 6.33 M KOH, 1.77 M and 5 M KOH solutions) and is the worst scenario with low capacities and high degradations.

Area 4: normalized degradation <100% and normalized capacity <100%. It contains additives with reduced chemical activity resulting in reduced capacity and degradation such as  $\text{NaCl}$  (0.44 M and 6.33 M KOH, 0.88 M and 5.88 M KOH, 1.33 M and 5.44 M KOH, 1.77 M and 5 M KOH solutions),  $\text{KNO}_3$  (0.44 M and 6.33 M KOH, 0.88 M and 5.88 M KOH solutions),  $\text{RbNO}_3$  (0.44 M and 6.33 M KOH solution),  $\text{LiNO}_3$  (0.44 M and 6.33 M KOH solution),  $\text{NaNO}_3$  (0.44 M and 6.33 M KOH solution),  $\text{RbCl}$  (0.44 M and 6.33 M KOH, 1.77 M and 5 M KOH solutions),  $\text{LiCl}$  (1.33 M and 5.44 M KOH, 1.77 M and 5 M KOH solutions), KI (0.88 M and 5.88 M KOH, 1.33 M and 5.44 M KOH, 1.77 M and 5 M KOH solutions),  $\text{K}_2\text{CO}_3$  (1.77 M and 5 M KOH solution),  $\text{KCHO}_2$  (0.44 M and 6.33 M KOH solution),  $\text{LiCHO}_2$  (0.44 M and 6.33 M KOH solution), KCl (0.88 M and 5.88 M KOH, 1.33 M and 5.44 M KOH solutions), CsCl (0.44 M and 6.33 M KOH, 0.88 M and 5.88 M KOH, 1.33 M and 5.44 M KOH, 1.77 M and 5 M KOH solutions),  $\text{K}_2\text{SO}_4$  (0.44 M and 6.33 M KOH solution),  $\text{Na}_2\text{SO}_4$  (0.44 M and 6.33 M KOH solution),  $\text{Na}_2\text{CO}_3$  (0.44 M and 6.33 M KOH solution),  $\text{Li}_2\text{SO}_4$  (0.005 M and 6.33 M KOH solution), and  $\text{CsCHO}_2$  (0.44 M and 6.33 M KOH solution).

In order to gain a better understanding of the effects of the anions and cations of additive salts on the normalized discharge capacity and electrode degradation, the data in Figure 3 was further analyzed based on the anions and cations.

### 3.3.3. Performance of Alkaline Cations Containing Electrolytes

Figures 4 and 5 illustrate the effects of alkaline cations (Li, Na, K, Rb, and Cs) on normalized degradation and discharge capacity, respectively, at 0.44 M of salt (with 6.33 M KOH), 0.88 M of salt (with 5.88 M KOH), 1.33 M of salt (with 5.44 M KOH), and 1.77 M of salt (with 5 M KOH). Figure 4 shows that degradation values vary from 26% to 115% with the addition of alkaline salts to traditional KOH electrolytes. CsCl and NaCl containing electrolytes decrease significantly in degradation compared to that in a pure KOH solution. At a low salt concentration (0.44 M salt with 6.33 M KOH), KCl containing electrolyte has a similar degradation value to KOH; LiCl containing electrolyte has an increased degradation, which is unfavorable; and RbCl electrolyte has a decreased degradation. At a high salt concentration (1.77 M salt with 5 M KOH), all electrolytes have a decreased degradation. Figure 5 illustrates that, except for NaCl containing electrolytes, the discharge capacity for electrolytes with a low salt concentration (0.44 M salt with 6.33 M KOH) is increased, while the discharge capacity for electrolytes with a high salt concentration (1.77 M salt with 5 M KOH) is greatly decreased. Figures 4 and 5 show that the concentration of alkaline salt in electrolytes has a significant influence on the degradation and discharge capacity. A linear correlation between degradation and reduction potential of alkaline ions was found for electrolytes containing a low concentration of salt, shown in Figure 6. It suggests that degradation is influenced by the reducibility of the salt additive. There is no apparent relationship between capacity and reduction potential of alkaline metals. There is also no apparent relationship between degradation and reduction potential in the electrolytes with high salt concentration. It is supposed that the high concentration of salt would cause the effect of electrostatic interaction among ions to become stronger and influence the degradation performance.

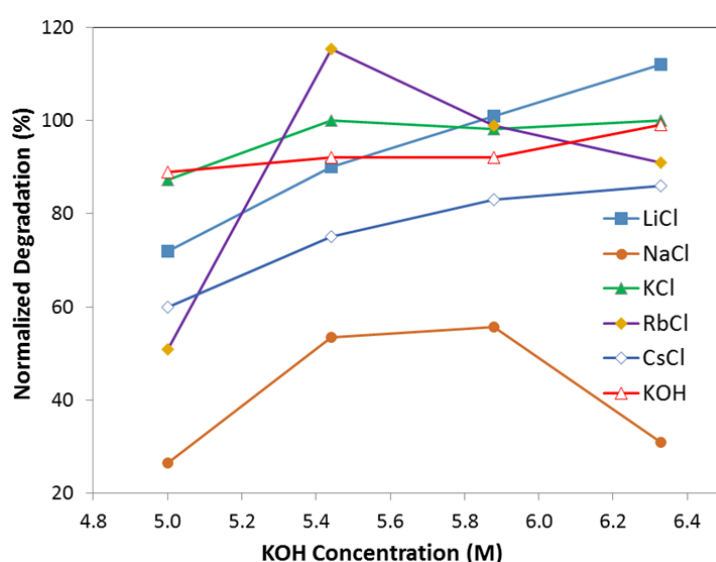


**Figure 4.** Degradation of electrolyte with 6.33 M KOH (and 0.44 M salts), 5.88 M KOH (and 0.88 M salts), 5.44 M KOH (and 1.33 M salts), 5.00 M KOH (and 1.77 M salts). Salts are LiCl, NaCl, KCl, RbCl, and CsCl, respectively.

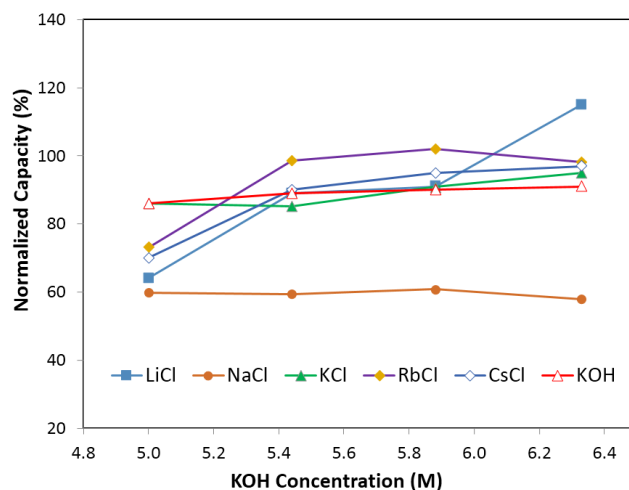


**Figure 5.** Capacity of electrolyte with 6.33 M KOH (and 0.44 M salts), 5.88 M KOH (and 0.88 M salts), 5.44 M KOH (and 1.33 M salts), 5.00 M KOH (and 1.77 M salts). Salts are LiCl, NaCl, KCl, RbCl, and CsCl, respectively.

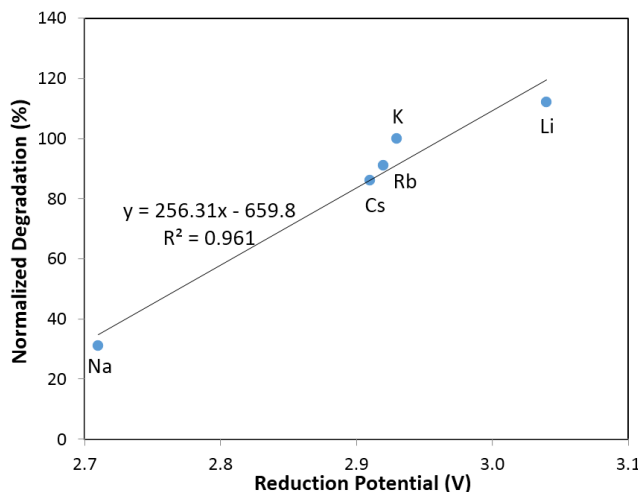


**Figure 6.** Linear fit of degradation with reduction potential of alkaline ions ( $\text{Li}^+$ ,  $\text{Na}^+$ ,  $\text{K}^+$ ,  $\text{Rb}^+$  and  $\text{Cs}^+$ ).

### 3.3.4. Performance of Halogen Containing Electrolytes

Figures 7 and 8 illustrate the effects of anions (F, Cl, Br and I) on normalized degradation and discharge capacity, respectively, with 0.44 M of salt (with 6.33 M KOH), 0.88 M of salt (with 5.88 M KOH), 1.33 M of salt (with 5.44 M KOH), and 1.77 M of salt (with 5 M KOH). Figure 7 illustrates that the normalized degradation varies from 78% to 105%, which suggests that halogen ions' effects on degradation is not as strong as those in alkaline ions'. Figure 7 also indicates that at low (0.44 M) and high salt concentrations (1.77 M), the additives slightly increase the degradation value except for the electrolyte with 0.44 M KF and 6.33 M KOH. Figure 8 illustrates that discharge capacity varies from 68% to 133%. At a low salt concentration (0.44 M salt and 6.33 M KOH), all salts boost the discharge capacity, and at a high salt concentration (1.77 M salt and 5 M KOH), only KF and KBr additives enhance the discharge capacity. Figures 7 and 8 indicate that the concentration of salt additive in the electrolyte has a significant influence on the electrochemical performance. Figure 9

shows an apparent correlation between anion radii and the normalized degradation of low salt concentration electrolytes (0.44 M salt and 6.33 M KOH). This finding can also be explained by the energies of H–F, H–Cl, H–Br, and H–I bonds. In the traditional KOH electrolyte system, the OH group is an effective carrier for proton transfer between electrodes. In the salt containing electrolytes, both the OH groups and salt anions act as proton carriers. As F has a smaller radius than Cl, Br and I, its bond energy of H–F at 135  $\text{kcal}\cdot\text{mol}^{-1}$  is higher than that of O–H at 111  $\text{kcal}\cdot\text{mol}^{-1}$ , H–Cl at 103  $\text{kcal}\cdot\text{mol}^{-1}$ , H–Br at 87.5  $\text{kcal}\cdot\text{mol}^{-1}$ , and H–I at 71  $\text{kcal}\cdot\text{mol}^{-1}$ . The H–F bond is more stable than other hydrogen–halogen bonds during the charge/discharge process. Therefore, KF shows a decreased degradation compared to other potassium halogen salts. The bond energies of H–Cl, H–Br, and H–I are less than O–H, which implies that in KCl, KBr, and KI containing electrolytes, the  $\text{OH}^-$  group is preferred as the proton accepter instead of  $\text{Cl}^-$ ,  $\text{Br}^-$  and  $\text{I}^-$ . Thus, KCl, KBr, and KI containing electrolytes (with a low salt concentration) show a higher degradation than the traditional KOH electrolyte.

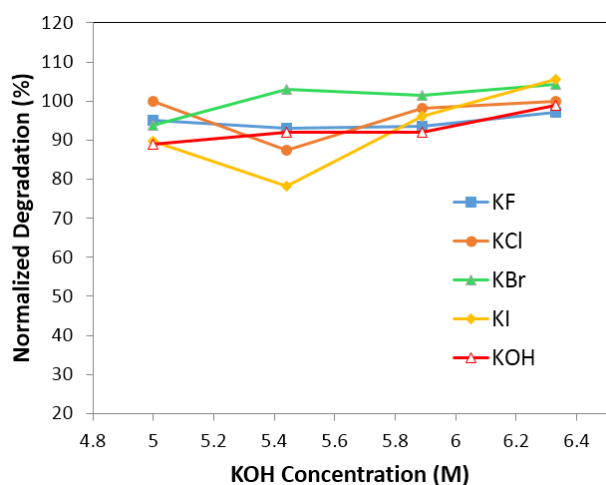


**Figure 7.** Degradation of electrolyte with 6.33 M KOH (and 0.44 M salts), 5.88 M KOH (and 0.88 M salts), 5.44 M KOH (and 1.33 M salts), 5.00 M KOH (and 1.77 M salts). Salts are KF, KCl, KBr, and KI, respectively.

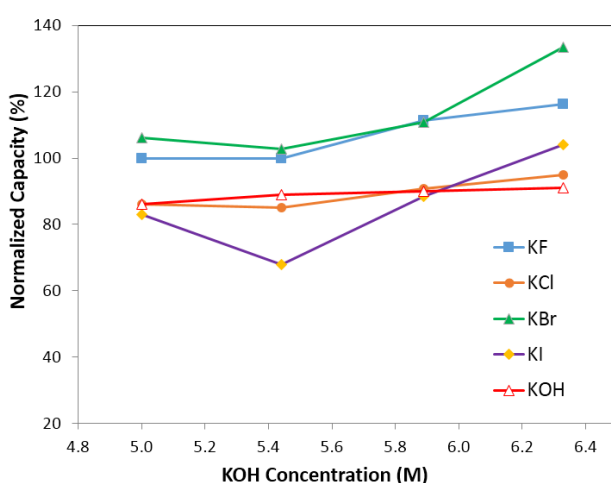


**Figure 8.** Capacity of electrolyte with 6.33 M KOH (and 0.44 M salts), 5.88 M KOH (and 0.88 M salts), 5.44 M KOH (and 1.33 M salts), 5.00 M KOH (and 1.77 M salts). Salts are KF, KCl, KBr, and KI, respectively.

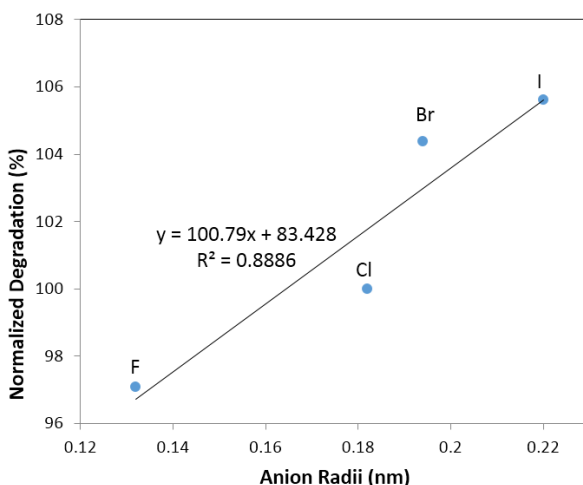


**Figure 9.** Linear fit of degradation with halogen anion radii ( $\text{F}^-$ ,  $\text{Cl}^-$ ,  $\text{Br}^-$ , and  $\text{I}^-$ ).

### 3.3.5 Performance of Oxyacid Containing Electrolytes

Effects of low oxyacid salt concentration (and 6.33 M KOH) electrolytes on normalized discharge capacity and degradation are shown in Figure 10. Unlike halogen salt additives and alkaline salt additives, all oxyacid salt additives satisfy the desired properties of degradation <100%, and distribute only in Areas 1 and 4. The electrolytes in Area 1 (*i.e.*, normalized degradation <100% and normalized discharge capacity >100%) include:  $\text{NaC}_2\text{H}_3\text{O}_2$  (0.44 M additives and 6.33 M KOH),  $\text{KC}_2\text{H}_3\text{O}_2$  (0.44 M additives and 6.33 M KOH),  $\text{K}_2\text{CO}_3$  (0.29 M additives and 6.33 M KOH),  $\text{Rb}_2\text{CO}_3$  (0.29 M additives and 6.33 M KOH),  $\text{Cs}_2\text{CO}_3$  (0.29 M additives and 6.33 M KOH),  $\text{K}_3\text{PO}_4$  (0.22 M additives and 6.33 M KOH),  $\text{Na}_2\text{WO}_4$  (0.29 M additives and 6.33 M KOH),  $\text{Rb}_2\text{SO}_4$  (0.005 M additives and 6.33 M KOH),  $\text{Cs}_2\text{SO}_4$  (0.005 M additives and 6.33 M KOH). The electrolytes in Area 4 (*i.e.*, normalized degradation <100% and normalized discharge capacity <100%) include:  $\text{Rb}_2\text{SO}_4$  (0.005 M additives and 6.33 M KOH),  $\text{Li}_2\text{SO}_4$  (0.005 M additives and 6.33 M KOH),  $\text{Rb}_2\text{SO}_4$  (0.005 M additives and 6.33 M KOH),  $\text{CsCHO}_2$  (0.44 M additives and 6.33 M KOH),  $\text{KNO}_3$  (0.44 M additives and 6.33 M KOH),  $\text{RbNO}_3$  (0.44 M additives and 6.33 M KOH),  $\text{LiNO}_3$  (0.44 M additives and 6.33 M KOH),  $\text{NaNO}_3$  (0.44 M additives and 6.33 M KOH),  $\text{K}_2\text{CO}_3$  (1.77 M additives and 5 M KOH),  $\text{KCHO}_2$  (0.44 M additives and 6.33 M KOH),  $\text{LiCHO}_2$  (0.44 M additives and 6.33 M KOH),  $\text{K}_2\text{SO}_4$  (0.005 M additives and 6.33 M KOH),  $\text{Na}_2\text{SO}_4$  (0.005 M additives and 6.33 M KOH), and  $\text{Na}_2\text{CO}_3$  (0.44 M additives and 6.33 M KOH).

The trend of discharge capacity is  $\text{NO}_3^- < \text{IO}_4^- < \text{CHO}_2^- < \text{SO}_4^{2-} < \text{WO}_4^{2-} < \text{CO}_3^{2-} < \text{PO}_4^{2-} < \text{C}_2\text{H}_3\text{O}_2^-$ . As shown in references [20,21], all of the above oxyacid anions, except for  $\text{NO}_3^-$ , could react with Mg or Ni ions on the surface of the metal hydride to form a solid layer that covers the metal hydride particles, which could protect them from electrolyte corrosion. The solid layer covering the metal hydride particles had a significant influence on discharge capacity and degradation. Figure 11 illustrates the charge voltage curves of the first cycle of cells with electrolytes containing  $\text{K}_2\text{CO}_3$ ,  $\text{K}_3\text{PO}_4$ ,  $\text{CsCO}_3$ ,  $\text{Rb}_2\text{CO}_3$ ,  $\text{Na}_2\text{WO}_4$ ,  $\text{NaC}_2\text{H}_3\text{O}_2$ ,  $\text{KC}_2\text{H}_3\text{O}_2$ ,  $\text{Rb}_2\text{SO}_4$ , and  $\text{Cs}_2\text{SO}_4$ , which demonstrated normalized degradation <100% and discharge capacity >100%. The full charge voltage of these oxyacid salt electrolytes is slightly lower than that of traditional KOH electrolyte, which means the resistance of these additive containing electrolytes is lower than that of traditional KOH electrolytes.

A lower voltage also implies less corrosion to the electrodes. The charge voltage curves of other salt additive containing electrolytes (in Areas 2, 3, and 4 in Figure 3) were also studied. The values of the first cycle full charge voltage were generally higher than that of KOH electrolyte (data not shown). Further research on the formation mechanism of solid layer and the effects of solid layer on corrosion resistance and electrochemical performance will be performed.

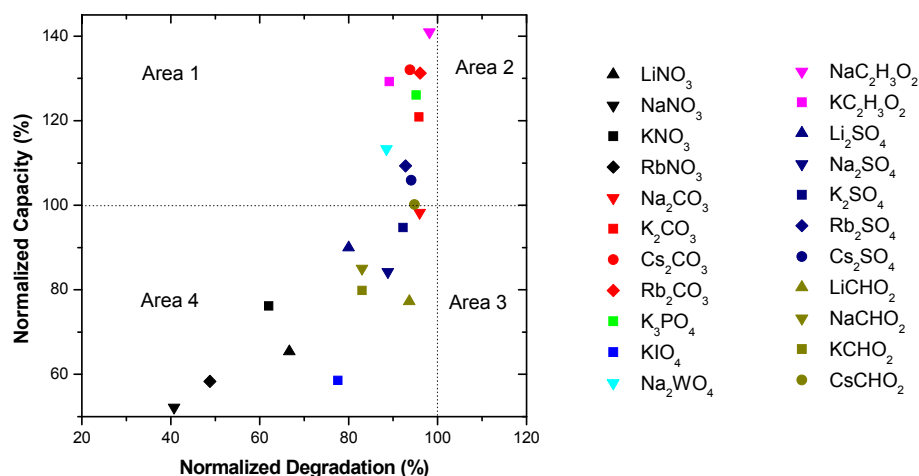


**Figure 10.** Discharge capacity and degradation for electrolytes containing oxyacid salts, including NaC<sub>2</sub>H<sub>3</sub>O<sub>2</sub>, KC<sub>2</sub>H<sub>3</sub>O<sub>2</sub>, K<sub>2</sub>CO<sub>3</sub>, Rb<sub>2</sub>CO<sub>3</sub>, Cs<sub>2</sub>CO<sub>3</sub>, K<sub>3</sub>PO<sub>4</sub>, Rb<sub>2</sub>SO<sub>4</sub>, Cs<sub>2</sub>SO<sub>4</sub>, Rb<sub>2</sub>CO<sub>3</sub>, Li<sub>2</sub>SO<sub>4</sub>, Rb<sub>2</sub>SO<sub>4</sub>, CsCHO<sub>2</sub>, KNO<sub>3</sub>, RbNO<sub>3</sub>, LiNO<sub>3</sub>, NaNO<sub>3</sub>, K<sub>2</sub>CO<sub>3</sub>, KCHO<sub>2</sub>, LiCHO<sub>2</sub>, K<sub>2</sub>SO<sub>4</sub>, Na<sub>2</sub>SO<sub>4</sub>, and Na<sub>2</sub>CO<sub>3</sub>.

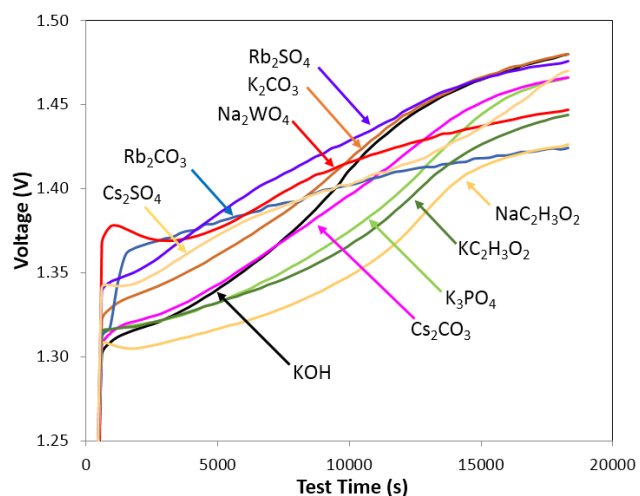


**Figure 11.** Charge voltage curves for first circle of electrolytes containing 0.29 M K<sub>2</sub>CO<sub>3</sub> and 6.33 M KOH, 0.29 M Cs<sub>2</sub>CO<sub>3</sub> and 6.33 M KOH, 0.29 M Rb<sub>2</sub>CO<sub>3</sub> and 6.33 M KOH, 0.29 M Na<sub>2</sub>WO<sub>4</sub> and 6.33 M KOH, 0.44 M NaC<sub>2</sub>H<sub>3</sub>O<sub>2</sub> and 6.33 M KOH, 0.44 M KC<sub>2</sub>H<sub>3</sub>O<sub>2</sub> and 6.33 M KOH, 0.005 M Rb<sub>2</sub>SO<sub>4</sub> and 6.33 M KOH, 0.005 M Cs<sub>2</sub>SO<sub>4</sub> and 6.33 M KOH, 0.22 M K<sub>3</sub>PO<sub>4</sub>, and 6.33 M KOH. The final charge voltage of these oxyacid salt containing electrolytes is lower than traditional KOH electrolyte.

Figure 12 shows the effects of K<sub>2</sub>CO<sub>3</sub> and K<sub>3</sub>PO<sub>4</sub> containing electrolytes on the normalized discharge capacity and degradation. It was found that the concentration of oxyacid salts, similar to the concentration

of halogen salts and alkaline salts, have a significant influence on electrochemical performance. There was a maximum value in discharge capacity for both 0.44 M  $K_2CO_3$  and  $K_3PO_4$  containing KOH electrolytes. On the other hand, the normalized degradation seemed to be stable for the concentration range of  $K_2CO_3$  and  $K_3PO_4$  studied, except for 0.89 M  $K_2CO_3$  containing electrolytes which shows a lower normalized degradation.

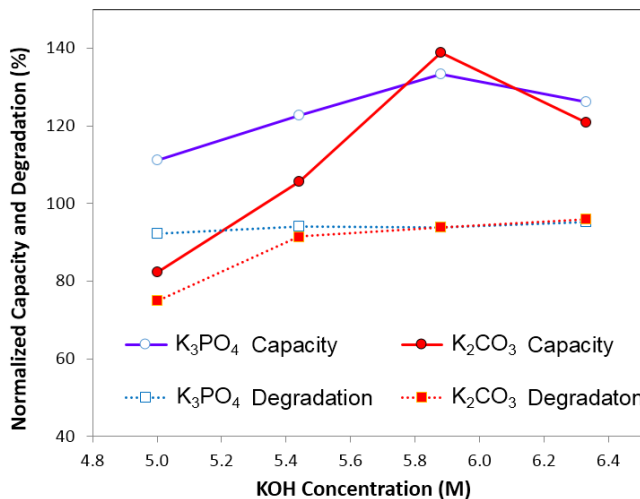


**Figure 12.** Degradation and capacity of the electrolytes containing  $K_2CO_3$  and  $K_3PO_4$  separately. The solutions are: 6.33 M KOH and 0.29 M  $K_2CO_3$ , 5.88 M KOH and 0.59 M  $K_2CO_3$ , 5.44 M KOH and 0.89 M  $K_2CO_3$ , 5.00 M KOH and 1.18 M  $K_2CO_3$ ; 6.33 M KOH and 0.22 M  $K_3PO_4$ , 5.88 M KOH and 0.44 M  $K_3PO_4$ , 5.44 M KOH and 0.66 M  $K_3PO_4$ , 5.00 M KOH, and 0.88 M  $K_3PO_4$ .

Since the electrolyte with 0.44 M  $Cs_2CO_3$  and 6.33 M KOH shows good performance on MgNi metal alloy, it was selected to test two kinds of BCC/C14 type metal alloy ( $V_{44.0}Ti_{15.6}Ni_{18.5}Cr_{11.6}Mn_{6.9}Hf_{2.1}Co_{1.4}Al_{0.4}$  and  $V_{44.0}Ti_{15.6}Ni_{18.5}Cr_{11.6}Mn_{6.9}Zr_{2.1}Co_{1.4}Al_{0.4}$ ). The BCC/C14 metal alloy has high hydrogen storage ability and high theoretical discharge capacity, and is also considered as a strong candidate material for metal alloy electrode in NiMH batteries as the MgNi metal alloy [7,8]. The theoretical discharge capacity of MgNi alloy ( $Mg_{52}Ni_{39}Co_3Mn_6$ ) was reported as  $999\text{ mAh}\cdot\text{g}^{-1}$  [7,10]. However, Figure 13 shows that the maximum value of practical discharge capacity in traditional 6.77 M KOH electrolyte over  $Mg_{52}Ni_{39}Co_3Mn_6$  is only  $212\text{ mAh}\cdot\text{g}^{-1}$ . When  $Mg_{52}Ni_{39}Co_3Mn_6$  alloy electrode is tested in  $Cs_2CO_3$  containing electrolyte, the maximum discharge capacity is  $300\text{ mAh}\cdot\text{g}^{-1}$ , which suggests less corrosive in  $Cs_2CO_3$  containing electrolyte. The theoretical discharge capacity of these two BCC/C14 alloys ( $V_{44.0}Ti_{15.6}Ni_{18.5}Cr_{11.6}Mn_{6.9}Hf_{2.1}Co_{1.4}Al_{0.4}$  and  $V_{44.0}Ti_{15.6}Ni_{18.5}Cr_{11.6}Mn_{6.9}Zr_{2.1}Co_{1.4}Al_{0.4}$ ) was reported as  $767\text{ mAh}\cdot\text{g}^{-1}$  [13]. In traditional 6.77 M KOH, the maximum capacity for  $V_{44.0}Ti_{15.6}Ni_{18.5}Cr_{11.6}Mn_{6.9}Hf_{2.1}Co_{1.4}Al_{0.4}$  is only  $348\text{ mAh}\cdot\text{g}^{-1}$  and capacity decay after 86 cycles' running is 78% and for  $V_{44.0}Ti_{15.6}Ni_{18.5}Cr_{11.6}Mn_{6.9}Zr_{2.1}Co_{1.4}Al_{0.4}$ , the maximum is  $366\text{ mAh}\cdot\text{g}^{-1}$  and capacity decay is 52%. In electrolyte of 0.44 M  $Cs_2CO_3$  and 6.33 M KOH, the maximum capacity of  $V_{44.0}Ti_{15.6}Ni_{18.5}Cr_{11.6}Mn_{6.9}Hf_{2.1}Co_{1.4}Al_{0.4}$  and  $V_{44.0}Ti_{15.6}Ni_{18.5}Cr_{11.6}Mn_{6.9}Zr_{2.1}Co_{1.4}Al_{0.4}$  is  $378\text{ mAh}\cdot\text{g}^{-1}$ . In addition, capacity decay of 100 cycles' running for  $V_{44.0}Ti_{15.6}Ni_{18.5}Cr_{11.6}Mn_{6.9}Hf_{2.1}Co_{1.4}Al_{0.4}$  is 33%, and for

$V_{44.0}Ti_{15.6}Ni_{18.5}Cr_{11.6}Mn_{6.9}Zr_{2.1}Co_{1.4}Al_{0.4}$  is 30%. As stated above, traditional 6.77 M KOH is quite corrosive to metal alloys and leads to a very low practical discharge capacity. The  $Cs_2CO_3$  salt additive slightly improves discharge capacity and tremendously decreases capacity decay on electrodes of  $Mg_{52}Ni_{39}Co_3Mn_6$ ,  $V_{44.0}Ti_{15.6}Ni_{18.5}Cr_{11.6}Mn_{6.9}Hf_{2.1}Co_{1.4}Al_{0.4}$  and  $V_{44.0}Ti_{15.6}Ni_{18.5}Cr_{11.6}Mn_{6.9}Zr_{2.1}Co_{1.4}Al_{0.4}$  as shown in Figure 13.

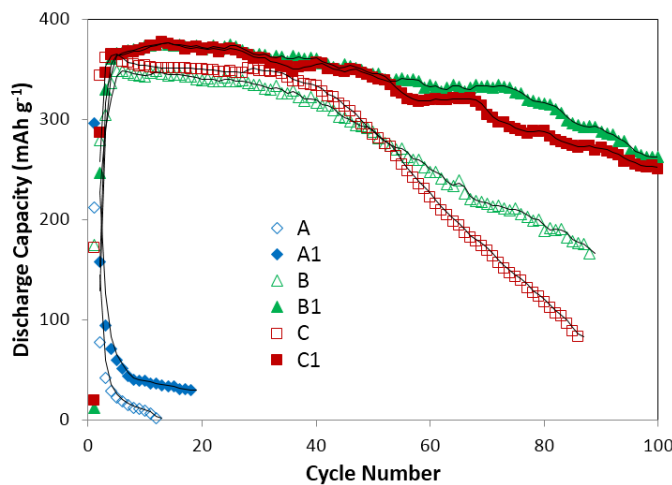


**Figure 13.** Discharge capacity of  $Mg_{52}Ni_{39}Co_3Mn_6$ ,  $V_{44.0}Ti_{15.6}Ni_{18.5}Cr_{11.6}Mn_{6.9}Hf_{2.1}Co_{1.4}Al_{0.4}$  and  $V_{44.0}Ti_{15.6}Ni_{18.5}Cr_{11.6}Mn_{6.9}Zr_{2.1}Co_{1.4}Al_{0.4}$  in electrolyte of 6.77 M KOH and electrolyte of 0.44 M  $Cs_2CO_3$  and 6.33 M KOH. A:  $Mg_{52}Ni_{39}Co_3Mn_6$  in 6.77 M KOH; B:  $V_{44.0}Ti_{15.6}Ni_{18.5}Cr_{11.6}Mn_{6.9}Hf_{2.1}Co_{1.4}Al_{0.4}$  in 6.77 M KOH; C:  $V_{44.0}Ti_{15.6}Ni_{18.5}Cr_{11.6}Mn_{6.9}Zr_{2.1}Co_{1.4}Al_{0.4}$  in 6.77 M KOH; A1:  $Mg_{52}Ni_{39}Co_3Mn_6$  in 0.44 M  $Cs_2CO_3$  and 6.33 M KOH; B1:  $V_{44.0}Ti_{15.6}Ni_{18.5}Cr_{11.6}Mn_{6.9}Hf_{2.1}Co_{1.4}Al_{0.4}$  in 0.44 M  $Cs_2CO_3$  and 6.33 M KOH; C1:  $V_{44.0}Ti_{15.6}Ni_{18.5}Cr_{11.6}Mn_{6.9}Zr_{2.1}Co_{1.4}Al_{0.4}$  in 0.44 M  $Cs_2CO_3$  and 6.33 M KOH. It shows  $Cs_2CO_3$  salt additive slightly improves discharge capacity and tremendously decreases capacity decay.

### 3.4. Mechanistic Analysis for Using Additive Containing Electrolytes in Novel Ni/MH Battery Systems

#### 3.4.1. Synergistic Effect between KOH and Salt Additives

Comparing additive containing electrolytes to the pure KOH and pure salt electrolytes, significant changes in degradation and discharge capacity were observed. For salts in Area 1 of Figure 3 (*i.e.*, degradation <100% and capacity >100%), a synergistic effect between the salt additives and KOH electrolyte is presumed to explain the improvement in electro-performance. The synergistic effect can be explained by the following inferences: (1) a solid film forms on the surface of both electrodes. As shown in Figure 14, all the anions in Area 1 were able to react with  $Mg^{2+}$  and  $Ni^{2+}$  on the surface of  $MgNi$  metal hydride particles and  $Ni^{2+}$  on the surface of  $\beta-Ni(OH)_2$  particles to form a solid deposit [20,21]. In this research, discharge capacity is closely related to the amount of  $MgNi$  metal hydride in negative electrodes. This solid film over the  $MgNi$  metal hydride particles could physically protect the electrode from electrolyte corrosion; (2) H-transfer is promoted in aqueous electrolyte. The salt additives' effects were considered from the aspects of the anions and cations. The anions of salts in

Area 1 could provide more active sites for H adsorption and transfer [22,23]. The cations, together with their anions, could change the chemical environment of the OH group in the electrolyte, and promote H-transfer [22]. Lower degradation is closely related to the improvement in the amount of H carriers and the H-transfer process [7].

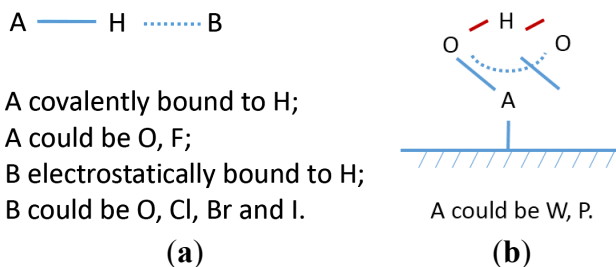


**Figure 14.** (a) Hydrogen bond types in additive containing H bond type 1; and (b) H bond type 2.

### 3.4.2. Active Sites for Proton Transfer and H Bond Types

For traditional KOH electrolytes, the oxygen atom in the  $\text{OH}^-$  group acts as the basic site to accept H from the metal hydride and transfers H between electrodes [22,24]. As Basak [22] stated, H is covalently bonded to O with bond energy around  $111 \text{ kcal}\cdot\text{mol}^{-1}$  and simultaneously has a weaker electrostatic interaction with another O with bond energy around  $6\text{--}10 \text{ kcal}\cdot\text{mol}^{-1}$ . This H bond type in KOH electrolytes is called H bond type 1 (shown in Figure 14a).

In this research, the anions of the additive salts, together with  $\text{OH}^-$  from KOH, act as proton carriers [22–25]. For halogen containing salts,  $\text{F}^-$ ,  $\text{Cl}^-$ ,  $\text{Br}^-$  and  $\text{I}^-$  are basic sites for H adoption [24,25]. H bond type in halogen containing electrolytes can be presumed by analyzing the bond energy [24]. The H–F bond energy is  $135 \text{ kcal}\cdot\text{mol}^{-1}$ , which is higher than O–H at  $111 \text{ kcal}\cdot\text{mol}^{-1}$ . Thus, F should be covalently bonded to H (as the A atom in Figure 14a), and OH should be electrostatically bonded to H (as the B atom in Figure 14b). The bond energies for H–Cl, H–Br, and H–I are 103, 87.5, and  $71 \text{ kcal}\cdot\text{mol}^{-1}$ , respectively, which are lower than the O–H bond energy. Thus, Cl, Br, or I should be electrostatically bonded to H (as the B atom in Figure 14a), and OH covalently bonded to H (as the A atom in Figure 14a) [24].

For most oxyacid salts, O is the basic site for H adsorption [22,24]. Analysis of the bonds containing O is important for understanding the H bond type in oxyacid salts. For  $\text{CO}_3^{2-}$ ,  $\text{C}_2\text{H}_3\text{O}_2^-$ , and  $\text{CHO}_2^-$  salts, there are two types of O containing bonds: C–O, and C=O. H is covalently bonded to C–O, and electrostatically bonded to C=O [24].  $\text{WO}_4^{2-}$  and  $\text{PO}_4^{3-}$  are special cases regarding H bond type. There are two identical W–O bonds and two identical W=O bonds in  $\text{WO}_4^{2-}$  and three identical P–O bonds in  $\text{PO}_4^{3-}$ . As Basak [22] stated, because of the identicity of the bonds, H is equally shared between two adjacent O by covalent interaction. In this paper, it is called H bond type 2, and its structure is as shown in Figure 14b.

### 3.4.3. Proton Transfer Mechanisms: Vehicle Mechanism and Structure-Diffusion Mechanism

Generally speaking, there are two kinds of proton transfer mechanisms in organic/inorganic solution systems: vehicle mechanism and structure-diffusion mechanism [22–25]. Vehicle mechanism

is reported in traditional KOH electrolytes and is described as the transport of protonated species as whole molecules (for example:  $\text{H}_2\text{O}$ ,  $\text{H}_3\text{O}^+$ ) through aqueous media [24]. In this research, proton transfer in liquid electrolyte is considered as vehicle mechanism. In addition, proton transfer through the surface solid of the electrodes, is considered as a structure-diffusion mechanism [22]. The proton hops from site to site along a hydrogen-bonded network over the surface. Diffusion of protonic charges or protonic defects occurs through the formation and breaking of the hydrogen bonds. Both H bond types could contribute to structure-diffusion mechanism.

The H-transfer process in additive containing electrolytes during discharge is briefly illustrated in Figure 15. The solid film over the MgNi alloy and  $\text{Ni(OH)}_2$  particles is formed during the charge process or the first few seconds of the discharge process. In the solid film covering the MgNi alloy, H is covalently or electrostatically bonded to other heteroatoms through bond type 1 or 2. H delivered through the solid film to the interface of the liquid electrolyte is through site-to-site hopping way (*i.e.*, structure-diffusion mechanism). The H is delivered in the electrolyte through vehicle mechanism with H bond type 1. The H bond type and H-transfer mechanism for the solid film covering the  $\text{Ni(OH)}_2$  are similar to that of the MgNi alloy. Figure 15 also illustrates the trend of the H concentration differential from the MgNi alloy to  $\text{Ni(OH)}_2$  during the discharge process. The H concentration is the highest at the metal hydride-solid film interface and the H concentration is the lowest at the  $\text{Ni(OH)}_2$ -solid film interface.

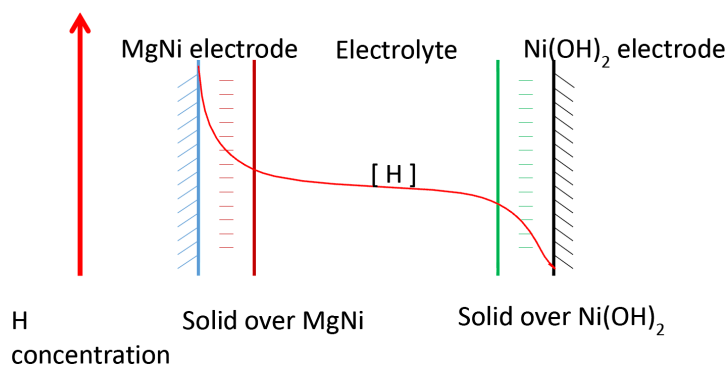


**Figure 15.** Model of H-transfer from the surface of MgNi electrode to  $\text{Ni(OH)}_2$  electrode through the novel additive containing electrolyte.

### 3.4.4. Factors that Influence Electrochemical Performance of the Novel Additive-Containing Electrolytes

As stated before, the synergy between the additives and KOH is influenced by the nature of the salt additives. For additive containing electrolytes, both hydroxide ions and salt anions are basic sites and act as proton acceptors and carriers [22]. Thus, the parameters that can influence the formation of hydrogen bonds can influence the electro-performance. The parameters are summarized as follows:

- (1) The nature of the basic sites. The stronger the basicity, the better the performance [23,24]. In this research,  $\text{CO}_3^{2-}$ ,  $\text{PO}_4^{3-}$ , and  $\text{F}^-$  are strong Lewis bases and do well in decreasing degradation and boosting discharge capacity.  $\text{NO}_3^-$  and  $\text{I}^-$  are weak Lewis bases and have poor hydrogen ion adsorption. In Figure 3,  $\text{NO}_3^-$  and  $\text{I}^-$  containing electrolytes show poor performance.
- (2) The amount of basic sites. Comparing  $\text{CHO}_2^-$  and  $\text{C}_2\text{H}_3\text{O}_2^-$  containing electrolytes, it was found that  $\text{C}_2\text{H}_3\text{O}_2^-$  shows better performance than  $\text{CHO}_2^-$ . For  $\text{CHO}_2^-$ , the Lewis basic site

that acts as the proton carrier is the oxygen in the C–O bond. For  $\text{C}_2\text{H}_3\text{O}_2^-$ , the Lewis basic sites include the oxygen in the C–O bond and the C from the  $\text{CH}_3^-$  group.  $\text{C}_2\text{H}_3\text{O}_2^-$  contains more basic sites than  $\text{CHO}_2^-$  [22].

- (3) The stability of the salt additives. During the charge/discharge processes, the salt additives are in highly reductive/oxidative environments. The additives with low stability, such as  $\text{KIO}_4$ , perform poorly.
- (4) The salt solubility in KOH solution. It has been found that all the  $\text{SO}_4^{2-}$  containing salts have low solubility in KOH solutions [20,21]. The maximum solubility of  $\text{K}_2\text{SO}_4$  in KOH is only around 0.093% (0.005 M). In this research, the  $\text{SO}_4^{2-}$  containing electrolyte performs poorly compared to other oxyacid salt electrolytes, and similarly to pure KOH solutions.
- (5) The ionic charge of the additive ions. Anions with high ionic charge, such as  $\text{CO}_3^{2-}$ ,  $\text{PO}_4^{3-}$ ,  $\text{WO}_4^{2-}$ , perform well.

#### 4. Conclusions

A systematic study of 32 salt additives in a traditional KOH electrolyte was performed on an MgNi-based Ni/MH battery systems. 12 salt additives were discovered to have efficiently decreased the corrosion of traditional KOH electrolyte:  $\text{NaC}_2\text{H}_3\text{O}_2$ ,  $\text{KC}_2\text{H}_3\text{O}_2$ ,  $\text{K}_2\text{CO}_3$ ,  $\text{Rb}_2\text{CO}_3$ ,  $\text{Cs}_2\text{CO}_3$ ,  $\text{K}_3\text{PO}_4$ ,  $\text{Na}_2\text{WO}_4$ ,  $\text{Rb}_2\text{SO}_4$ ,  $\text{Cs}_2\text{SO}_4$ ,  $\text{NaF}$ ,  $\text{KF}$ , and  $\text{KBr}$ .

The effects of the cations ( $\text{Li}^+$ ,  $\text{Na}^+$ ,  $\text{K}^+$ ,  $\text{Rb}^+$ , and  $\text{Cs}^+$ ) and anions ( $\text{F}^-$ ,  $\text{Cl}^-$ ,  $\text{Br}^-$ ,  $\text{I}^-$ ,  $\text{CO}_3^{2-}$ ,  $\text{NO}_3^-$ ,  $\text{PO}_4^{3-}$ ,  $\text{SO}_4^{2-}$ ,  $\text{IO}_4^-$ ,  $\text{WO}_4^{2-}$ ,  $\text{C}_2\text{H}_3\text{O}_2^-$ , and  $\text{CHO}_2^-$ ) of the additives on charge/discharge performance were discussed. It was found that the oxidation potential of alkaline ions and the radii of halogen ions are linearly correlated with electrode degradation. For oxyacid salt electrolytes, a synergistic effect between the salt and KOH was observed: (1) a solid film forms on the MgNi particle surface, which physically prevents corrosion from KOH electrolyte and boosts discharge capacity; (2) H-transfer is promoted in aqueous electrolyte, which decreases degradation.

A brief discuss for H-transfer in the additive containing electrolyte system was included based on the screen test data. H bond type in the novel electrolyte system is not similar to traditional KOH electrolyte. Both type 1 and 2 hydrogen bonds exist in the additives containing electrolytes. Because of the formation of the solid film on the MgNi particles, the H-delivery mechanism in the novel electrolyte is also different from traditional KOH electrolytes. Both vehicle mechanism and structure-diffusion mechanism occurred in the novel electrolyte system. As the synergistic effect is determined by the nature of the salt additive, the factors that could influence the electro-performance were discussed based on the salt additive's chemical properties including the salt's anion's basicity, amount of base sites, stability during charging/discharging, solubility in KOH solution, and ionic charge.

#### Acknowledgments

This work is financially supported by Advanced Research Projects Agency-Energy (ARPA-E) under the robust affordable next generation EV-storage (RANGE) program (DE-AR0000386).

## Conflicts of Interest

The authors declare no conflict of interest.

## References

1. Linden, D.; Reddy, T.B. *Handbook of Batteries*; McGraw-Hill: New York, NY, USA, 2002.
2. Fetcenko, M.A.; Ovshinsky, S.R.; Reichman, B.; Young, K.; Fierro, C.; Koch, J.; Zallen, A.; Mays, W.; Ouchi, T. Recent advances in NiMH battery technology. *J. Power Sources* **2007**, *165*, 544–551.
3. Iwakura, C.; Fukuda, K.; Senoh, H.; Inoue, H.; Matsuoka, M.; Yamamoto, Y. Electrochemical characterization of  $MmNi_{4.0-x}Mn_{0.75}Al_{0.25}Co_x$  electrodes as a function of cobalt content. *Electrochim. Acta* **1998**, *43*, 2041–2046.
4. Geng, M.; Feng, F.; Sebastian, P.J.; Matchett, A.J.; Northwood, D.O. Charge transfer and mass transfer reactions in the metal hydride electrode. *Int. J. Hydrot. Energy* **2001**, *26*, 165–169.
5. Niessen, R.A.H.; Notten, R.H.L. Electrochemical hydrogen storage characteristics of thin film  $MgX$  ( $X = Sc, Ti, V, Cr$ ) compounds. *Electrochem. Solid State Lett.* **2005**, *8*, 534–538.
6. Notten, P.H.L.; Ouwerkerk, M.; Hal, H.V.; Beelen, D.; Keur, W.; Zhou, J.; Fei, H. High energy density strategies: From hydride-forming materials research to battery integration. *J. Power Sources* **2004**, *129*, 45–54.
7. Young, K.; Nei, J. The current status of hydrogen storage alloy development for electrochemical applications. *Materials* **2013**, *6*, 4574–4608.
8. Anik, M.; Özdemir, G.; Küçükdeveci, N. Electrochemical hydrogen storage characteristics of Mg–Pd–Ni ternary alloys. *Int. J. Hydrot. Energy* **2011**, *36*, 6744–6750.
9. Rongeat, C.; Grosjean, M.H.; Ruggeri, S.; Dehmas, M.; Bourlot, S.; Marcotte, S.; Roué, L. Evaluation of different approaches for improving the cycle life of MgNi-based electrodes for Ni-MH batteries. *J. Power Sources* **2006**, *158*, 747–753.
10. Liu, J. Effect of Ti-La substitution on electrochemical properties of amorphous MgNi-based secondary hydride electrodes. *J. Tianjin Norm. Univ.* **2011**, *313*, 67–70.
11. Anik, M.; Özdemir, G.; Küçükdeveci, N.; Baksan, B. Effect of Al, B, Ti and Zr additive elements on the electrochemical hydrogen storage performance of MgNi alloy. *Int. J. Hydrot. Energy* **2011**, *36*, 1568–1577.
12. Kalinichenka, S.; Röntzsch, L.; Riedl, T.; Gemming, T.; Weißgärber, T.; Kieback, B. Microstructure and hydrogen storage properties of melt-spun Mg–Cu–Ni–Y alloys. *Int. J. Hydrot. Energy* **2011**, *36*, 1592–1600.
13. Ma, F.; Liu, X.; Yan, S.; Ao, D.; Ren, Y. Research progress of influence factors on electrochemical performance of Mg-base hydrogen storage alloys. *Met. Func. Mater.* **2011**, *34*, 63–64.
14. Anik, M. Effect of titanium additive element on the discharging behavior of MgNi alloy electrode. *Int. J. Hydrot. Energy* **2011**, *36*, 15075–15080.

15. Danczuk, M.; Nunes, C.V., Jr.; Araki, K.; Anaissi, F.J.J. Influence of Alkaline Cation on the Electrochemical Behavior of Stabilized Alpha Nickel Hydroxide. *Solid State Electron.* **2014**, *18*, 2279–2287.
16. Karwowska, M.; Jaron, T.; Fijalkowski, K.J.; Leszczynski, P.J.; Rogulski, Z.; Czerwinski, A. Influence of electrolyte composition and temperature on behaviour of AB<sub>5</sub> hydrogen storage alloy used as negative electrode in Ni–MH batteries. *J. Power Sources* **2014**, *263*, 304–309.
17. Shangguan, E.; Li, J.; Chang, Z.; Tang, H.; Li, B.; Yuan, X.; Wang, H. Sodium tungstate as electrolyte additive to improve high-temperature performance of nickel–metal hydride batteries. *Int. J. Hydrog. Energy* **2013**, *38*, 5133–5138.
18. Vaidyanathan, H.; Robbins, K.; Rao, G.M. Effect of KOH concentration and anions on the performance of an Ni-H<sub>2</sub> battery positive plate. *J. Power Sources* **1996**, *63*, 7–13.
19. Ovshinsky, S.R.; Fetcenko, M.A.; Reichman, B.; Young, K.; Chao, B.; Im, J. Electrochemical Hydrogen Storage Alloys and Batteries Fabricated from Mg containing Base Alloys. U.S. Patent 5,616,432, 1 April 1997.
20. Schlapbach, L.; Züttel, A. Hydrogen-storage materials for mobile applications. *Nature* **2001**, *414*, 353–358.
21. Zaluska, A.; Zaluski, L.; Ström-Olsen, J.O. Structure, catalysis and atomic reactions on the nano-scale: A systematic approach to metal hydrides for hydrogen storage. *Appl. Phys. A* **2001**, *72*, 157–165.
22. Basak, D. *Proton Transfer in Organic Scaffolds*; University of Massachusetts Amherst: Amherst, MA, USA, 2012.
23. Gilli, P.; Bertolasi, V.; Ferretti, V.; Gilli, G. Covalent nature of the strong homonuclear hydrogen bond—Study of the O–H---O system by crystal structure correlation methods. *J. Am. Chem. Soc.* **1994**, *116*, 909–915.
24. Grabowski, J.S. What is the covalency of hydrogen bonding? *Chem. Rev.* **2011**, *111*, 2597–2625.
25. Wang, B.C.; Chang, J.C.; Jiang, J.C.; Lin, S.H. Ab initio study of the ammoniated ammonium ions NH<sub>4</sub><sup>+</sup>(NH<sub>3</sub>)<sub>0–6</sub>. *Chem. Phys.* **2002**, *276*, 93–106.

© 2015 by the authors; licensee MDPI, Basel, Switzerland. This article is an open access article distributed under the terms and conditions of the Creative Commons Attribution license (<http://creativecommons.org/licenses/by/4.0/>).